RESEARCH ARTICLE

Macromolecular Rapid Communications
www.mrc-journal.de

Photo-Mediated RAFT Step-Growth Polymerization With Diacrylate Monomers: Investigating Versatility and Oxygen Tolerance

Samantha Marie Clouthier, Jiajia Li, Joji Tanaka, and Wei You**

Photomediated reversible addition fragmentation chain transfer (RAFT) step-growth polymerization is performed using a trithiocarbonate-based chain transfer agent (CTA) and acrylate-based monomers both with and without a photocatalyst. The versatility of photo-mediated RAFT step-growth is demonstrated by one-pot synthesis of a graft copolymer via sequential monomer addition. Furthermore, oxygen-tolerant photo-mediated RAFT step-growth is demonstrated, facilitated by the appropriate selection of photocatalyst and solvent pair (zinc tetraphenyl porphyrin [ZnTPP] and dimethyl sulfoxide [DMSO]), enabling ultralow volume polymerization under open-air conditions.

1. Introduction

Traditionally, radical polymerizations encounter oxygen intolerance, where oxygen inhibits polymerization by quenching the radicals and forming unwanted side products.[1] Consequently, the pursuit of oxygen-tolerant radical polymerizations has gained momentum,[2–8] enabling polymerization in novel contexts such as low volume and continuous flow systems.[3,8] Moreover, oxygen tolerance expands the applicability of polymerization to settings such as high throughput screening, 3D printing, and the production of photocurable polymers for dental applications,[4,9] which demands open-air environments.

The advent of oxygen-tolerant reversible deactivation radical polymerizations (RDRP), including oxygen-tolerant atom transfer radical polymerization (ATRP),[10,11] nitroxide-mediated polymerization (NMP),[12] and reversible addition-fragmentation chain transfer (RAFT),[2,6,13] underscores the growing interest in this area. A notable technique, photo-induced electron/energy transfer reversible addition-fragmentation chain transfer (PET-RAFT), offers a unique advantage, as it can operate in the presence of oxygen with the appropriate selection of photocatalyst and solvent, such as zinc tetraphenyl porphyrin (ZnTPP) and dimethyl sulfoxide (DMSO).[3] In such a system, ZnTPP converts triplet-state oxygen to its singlet state, which is then quenched by DMSO to form dimethyl sulfone ($DMSO_2$) (Scheme S1, Supporting Information). This oxygen scavenging mechanism eliminates the need for deoxygenation procedures and allows polymerization to proceed under open-air conditions, thus enhancing the user-friendliness of RAFT.

On the other hand, RAFT step-growth polymerization combines the advantageous features of high functional group tolerance and the user-friendly nature of RAFT with the versatility in backbone functionality from step-growth polymerization, yielding highly functional backbones.[14] Until now, RAFT step-growth has only been conducted under inert gas conditions, necessitating deoxygenation of reaction vials with inert gasses like argon prior to initiation.[14–19] Recently, we introduced photo-mediated RAFT step-growth polymerization techniques, employing both catalyst-free RAFT-iniferter conditions and PET-RAFT conditions, across various wavelengths of visible light with maleimidic monomers.[17] This extension of RAFT step-growth to milder conditions opens up exciting possibilities for interesting applications. However, maleimidic monomers exhibit limited solvent compatibility, either due to solubility issues[16,17] or uncontrollable behavior in polar solvents like DMSO.[14] Thus, there is a need to broaden the scope of photo-mediated RAFT step-growth beyond maleimidic monomers.

Recently, we demonstrate the feasibility of RAFT step-growth using diacrylate monomers, allowing polymerization in polar solvents like DMSO to proceed in a predictable fashion.[15] Here we extend photo-mediated RAFT step-growth to acrylic monomers, employing both photo-iniferter and PET-RAFT techniques. Furthermore, we showcase the robustness of PET-RAFT step-growth under open-air conditions (**Scheme 1**).

S. M. Clouthier, J. Li, J. Tanaka, W. You
Department of Chemistry
University of North Carolina at Chapel Hill
Chapel Hill, NC 27599-3290, USA
E-mail: joji@email.unc.edu; wyou@unc.edu
J. Li
State and Local Joint Engineering Laboratory for Novel Functional Polymeric Materials, Jiangsu Key Laboratory of Advanced Functional Polymer Design and Application, Department of Polymer Science and Engineering
College of Chemistry
Chemical Engineering and Materials Science
Soochow University
Suzhou 215123, China

The ORCID identification number(s) for the author(s) of this article can be found under https://doi.org/10.1002/marc.202400602

DOI: 10.1002/marc.202400602

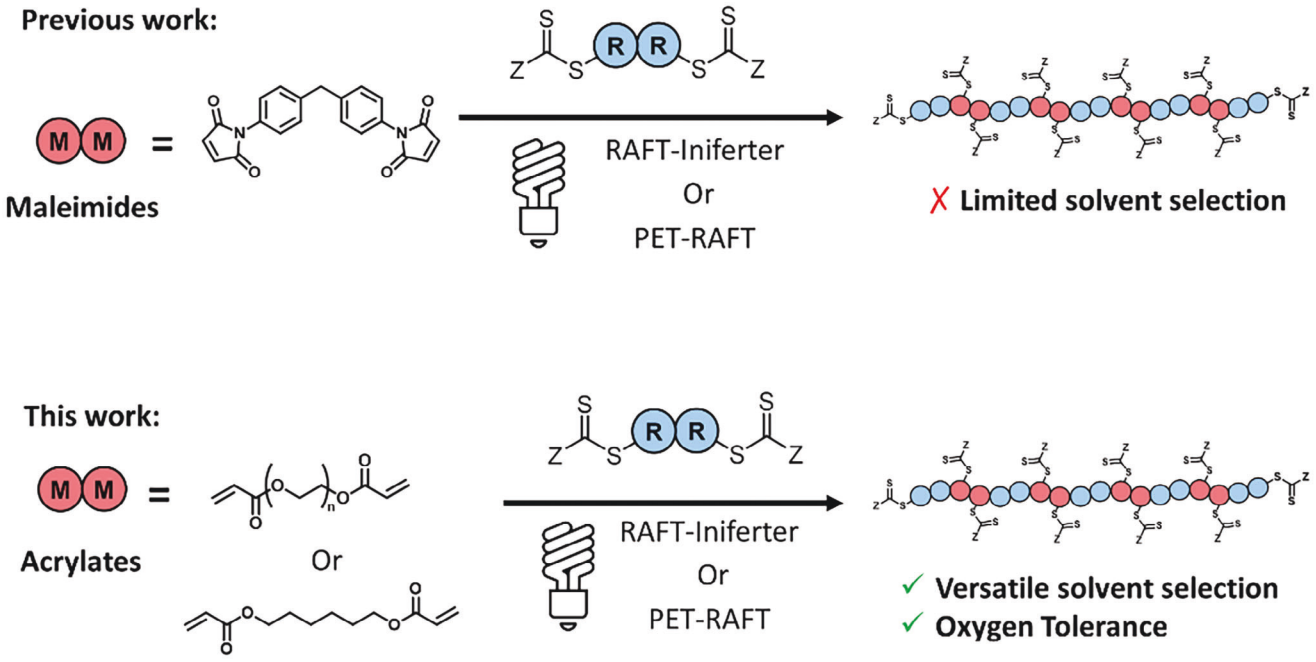

Scheme 1. Difference between our previous approach and our current approach in photomediated RAFT step-growth polymerization.

2. Results and Discussion

2.1. PET-RAFT Versus RAFT-Iniferter Step-Growth Polymerization of Diacrylates

We commenced our exploration of photo-mediated RAFT step-growth by polymerizing a bifunctional monomer (1,6 hexanediol diacrylate, $\mathbf{M_{2A}}$) with a bifunctional RAFT agent ($\mathbf{CTA_2}$). This was conducted under RAFT-iniferter conditions utilizing blue light (458 nm) and PET-RAFT conditions employing red light (625 nm) and ZnTPP as the photo-catalyst. These wavelengths were determined to be optimal for the respective polymerization conditions in our previous report (**Figure 1**).[17] Initially, the reaction mixture was prepared using a previously reported monomer concentration for diacrylates ($[M]_0 = 2.0$ M) in dimethyl formamide (DMF) for both photo-mediated conditions.[15] Additionally, in the case of PET-RAFT, the catalyst concentration was reduced to 2.5 mM ($[ZnTPP]_0 = 2.5$ mM) from our previous report in TCE to account for the lower solubility in DMF. ^{1}H-NMR was used to determine monomer conversion as previously reported and SEC analysis was used to determine the molecular weights relative to polystyrene standards in THF.[15]

As anticipated, the evolution of molecular weight averages (M_n, M_w, and M_z) with conversion aligned with the predictions of Flory's equations for linear step-growth polymerization under both PET-RAFT and RAFT-iniferter conditions (**Figure 1A**), using our photoreactors (Figure S1A, Supporting Information).[20] Notably, PET-RAFT step-growth exhibited significantly faster pseudo-first-order kinetics reaching high conversion within 8 h, compared to RAFT-iniferter step-growth (Figure 1B) where lower conversion was obtained after 24 h (Tables S1–S2 and Figures S2–S4, Supporting Information). While accelerated photo-mediated polymerization kinetics are expected in the presence of a photocatalyst, this is in contrast to our prior findings with bis-maleimides as the bifunctional monomer,[17] where faster kinetics were observed in the absence of the photocatalyst. In fact, we observed that photo-mediated RAFT step-growth of diacrylates proceeded with a faster rate compared to bis-maleimides under both PET-RAFT and RAFT-iniferter conditions using the same photo-reactors.[17] We have also conducted the RAFT-iniferter step-growth polymerization of diacrylates under green light irradiation; the resulting polymerization progressed at a comparable rate to blue light irradiation (Table S3 and Figures S5,S6, Supporting Information), and molecular weight averages (M_n, M_w, and M_z) followed the expected trend with conversion for step-growth (Figure S6), achieving high conversion and molecular weight after 24 h ($p > 97\%$, $M_w = 19.3$ k). It is worth noting that in our initial demonstration under blue light a slight high molecular weight shouldering was observed after 24 h in the SEC trace (Figure S4, Supporting Information), which is likely attributable to chain growth propagation.

2.2. One Pot Graft Copolymer Synthesis Via PET-RAFT Step-Growth Polymerization

To showcase the versatility of photo-mediated RAFT step-growth polymerization, we conducted a one-pot synthesis to prepare graft co-polymers via sequential monomer addition. This one-pot approach is different from our previous experiments where we purified the RAFT step-growth polymer backbone prior to polymerizing the grafting side chains.[14–17]

Following the same reaction conditions as described above, we first polymerized P(CTA_2-*alt*-M_{2A}) using PET-RAFT under red light in DMF, and achieved modest conversion and molecular weight after 8 h ($p = 93.8\%$, $M_n = 3$k) (**Figure 2**; Figure S7,

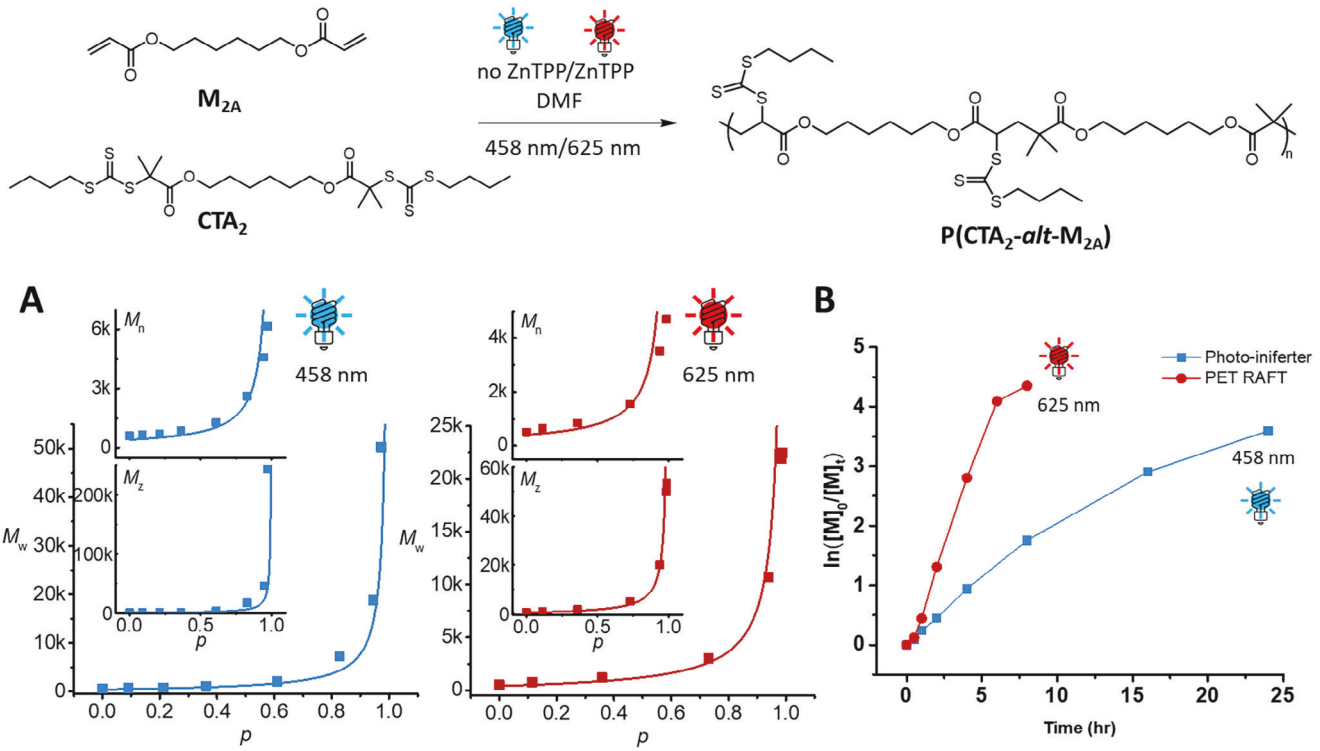

Figure 1. $A_2 + B_2$ photo-mediated RAFT step-growth polymerization with $\mathbf{M_{2A}}$ and $\mathbf{CTA_2}$. A) Evolution of the molecular weight averages (M_w, M_n, and M_z) from SEC analysis using polystyrene calibration, plotted with monomer conversion (p) determined by ^{1}H-NMR spectroscopy. These are plotted with the theoretical line for step-growth molecular weight evolution that assumes no cyclization.[20] B) Semi-logarithmic plot of RAFT-iniferter and PET-RAFT polymerization kinetics.

Supporting Information). Subsequently, without any purification step, we proceeded to graft poly(butyl acrylate) (PBA) from the pendant RAFT agents along the backbone via PET-RAFT controlled chain-growth polymerization. We attained 40% conversion after 8 h, using a monomer to CTA ratio of 40 ($[BA]_0/[CTA]_0 = 40$) (Figure 2; Figure S7, Supporting Information). The successful formation of the graft copolymer is evidenced by the shift in the molecular weight distribution (Figure 2). Interestingly, the presence of unreacted monomer end groups on the backbone did not lead to high molecular weight branching during the graft polymerization.

Continuing with the same monomers, we conducted a one-pot synthesis of graft copolymers in bulk under RAFT-iniferter conditions using blue light (Figures S8,S9, Supporting Information), resulting in modest molecular weight for both the backbone and graft co-polymer ($M_n = 5$k, $p = 98\%$ and $M_n = 7$k, $p = 35\%$, respectively). It is worth noting that this solvent-free ("green") condition was achievable due to the catalyst-free nature of RAFT-iniferter process and the liquid state of the polymer and the starting materials.

In our one-pot synthesis of graft co-polymers, we achieved a moderate number-average molecular weight. This outcome was influenced by the formation of oligomeric cyclic species during the step-growth polymerization process, a common occurrence with flexible bifunctional reagents. Furthermore, under bulk RAFT-iniferter conditions, the graft polymerization exhibited a high dispersity ($Đ = 5.08$). This is attributed to the presence of a low molecular weight tail and minor high molecular weight shoulder, which likely resulted from grafts initiated by low molecular weight oligomeric cyclic species and an increased occurrence of intermolecular coupling at high concentration. Despite this, it is important to highlight the simplicity and adaptability of this polymerization method.

2.3. Kinetics of PET-RAFT Step-Growth in Different Solvents

In our next step, we conducted a screening of various solvents to investigate the solvent dependency on PET-RAFT step-growth polymerization kinetics. Previous studies have indicated that PET-RAFT polymerization with ZnTPP in DMSO exhibits faster kinetics compared to other solvents (such as DMF), particularly in the context of controlled chain-growth polymerization.[5] However, it is worth noting that P(CTA_2-*alt*-M_{2A}) was found to be insoluble in DMSO, leading to phase separation in the reaction vial during polymerization.[15] Therefore we opted to utilize poly(ethylene glycol) diacrylate (PEGDA, $\mathbf{M_{2B}}$) as the bifunctional monomer to investigate the polymerization kinetics of PET-RAFT step-growth in DMSO, while simultaneously testing DMF, tetracholorethane (TCE), and 1,4-dioxane as alternative solvents (**Figure 3**).

As expected, the evolution of the molecular weight averages (M_n, M_w, and M_z) with conversion aligned well for linear step-growth as predicted by Flory's equations (Figure 3B) for all the solvents examined.[20] However, in certain cases, high molecular weight shouldering was apparent in SEC traces at high

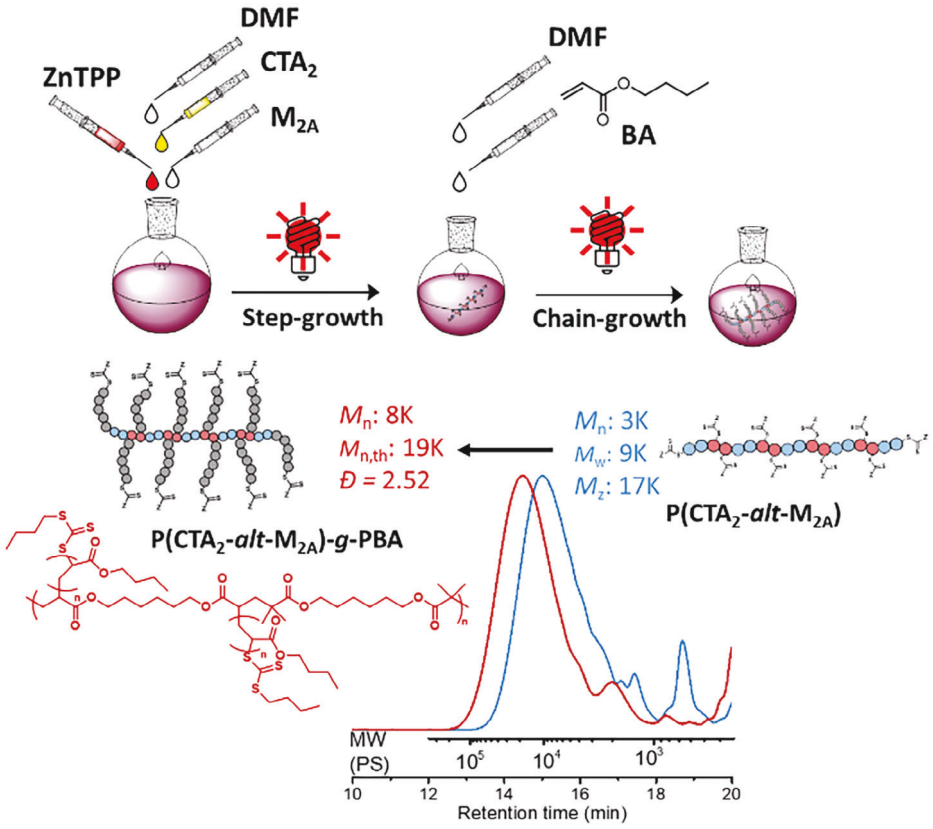

Figure 2. One-pot preparation of graft copolymers via photo-mediated RAFT step-growth.

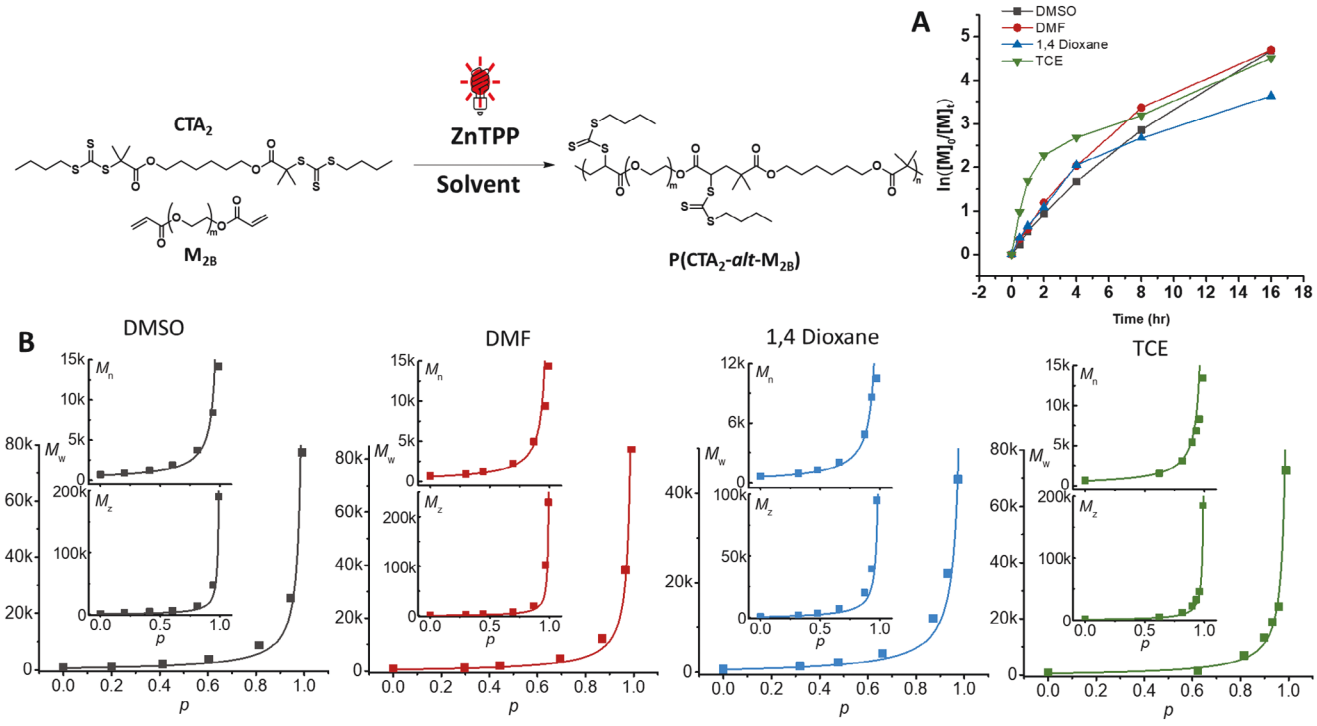

Figure 3. $A_2 + B_2$ PET-RAFT step-growth polymerization with $\mathbf{M_{2B}}$ and $\mathbf{CTA_2}$. A) Semi-logarithmic plot of polymerization kinetics for various solvents. B) Evolution of the molecular weight averages (M_w, M_n, and M_z) from SEC analysis using polystyrene calibration, plotted with monomer conversion (p) determined by ^{1}H-NMR spectroscopy. These are plotted with the theoretical line for step-growth molecular weight evolution that assumes no cyclization.[20]

conversion (Figure S14, Supporting Information), thus resulting in higher M_z relative to M_w than expected ($M_z/M_w = 1.5$ for ideal step-growth), which we again attribute to possible chain-growth propagation.

Interestingly, most of the solvents examined revealed comparable linear pseudo-first order kinetics (Figure 3A); however, to our surprise, the polymerization in TCE exhibited a significantly faster rate in the initial 2 h (p = 90% after 2.0 h) compared to the other solvents (p < 69% after 2 h for DMSO, DMF, and 1,4-dioxane) resulting in an early deviation in pseudo-first order kinetics (Table S4 and Figures S10–S14, Supporting Information). To further verify this peculiar kinetics of diacrylates in TCE, $\mathbf{M_{2A}}$ was then polymerized under the same conditions. A similar unexpected rapid rate deviating from pseudo-first order kinetics was observed with TCE, while DMF and 1,4-dioxane proceeded with the expected linear trend in pseudo-first order kinetics (Table S5 and Figures S15–S18, Supporting Information). While we acknowledge that the photocatalyst exhibits better solubility in TCE compared to the other solvents, it is worth mentioning that this trend was not observed with PET-RAFT step-growth of bismaleimides. Nonetheless, further investigation is warranted to delve into the intricacies of the polymerization kinetics in this system.

2.4. Oxygen Tolerant PET-RAFT Step-Growth

As mentioned previously, the use of ZnTPP as a photocatalyst in DMSO allows for PET-RAFT step-growth to be performed in the presence of oxygen, owing to the oxygen scavenging mechanism.[3] To investigate oxygen tolerance in PET-RAFT step-growth, $\mathbf{M_{2B}}$ was polymerized with $\mathbf{CTA_2}$ under similar conditions as above, without any deoxygenation procedures. Additionally, the reaction vial was fitted with a vent needle to ensure exposure to open air conditions, with an oxygen sensing probe monitoring the oxygen content in the headspace. The semi-logarithmic plot suggests that PET-RAFT proceeds much slower under open air conditions reaching slightly lower conversion (p = 95%) even after extended reaction time of 48 h, compared to 16 h in the absence of oxygen (where p > 99%) (**Figure 4B**). Nevertheless, the polymerization progressed in accordance with the expected step-growth molecular weight evolution with conversion predicted by Flory's equations (Figure 4A; Table S6 and Figures S19–S20, Supporting Information).[20] Additionally, the percent volume of oxygen readings remained constant during the polymerization (between 20% and 21%), confirming that a vent needle was sufficient to expose the polymerization to open-air environment (Figure 4B). Furthermore, we conducted the open-air polymerization in DMF to demonstrate the necessity of DMSO to scavenge oxygen, which resulted in insufficient monomer conversion (p = 81%) even after 48 h (Table S7 and Figures S21–S22, Supporting Information).

Interestingly, the kinetics for the open-air condition plateaued after 8 h, which we attribute to a drop in catalyst efficiency. To verify this, we examined the conversion of DMSO to $DMSO_2$ with ZnTPP in the absence of monomer and RAFT agent at various initial ZnTPP concentrations ($[ZnTPP]_0$ = 2.50, 1.25, and 0.625 mM) (Figure S23, Supporting Information). Under these conditions, the reaction rate appeared independent of both initial photocatalyst concentration ($[ZnTPP]_0$) and DMSO concentration ($[DMSO]_0$). For the reaction condition where $[ZnTPP]_0$ = 1.25 mM, more ZnTPP was added after 337 h (such that $[ZnTPP]_{t=337}$ = 2.50 mM), resulting in an increase in rate, suggesting a drop in catalyst efficiency after long irradiation times.

Next, we investigated the effect of monomer concentration on the polymerization while either keeping the initial photocatalyst concentration constant ($[ZnTPP]_0$ = 2.50 mM) or by maintaining the ratio of RAFT agent to photocatalyst constant ($[CTA]_0/[ZnTPP]_0$ = 400) (Tables S8–S9 and Figures S24–S32, Supporting Information). Interestingly, decreasing the monomer concentration to 0.5 M for both conditions resulted in faster polymerization kinetics, achieving higher molecular weight and conversion within 24 h (M_w > 30 k, p > 98%). Although lower molar monomer concentration is generally not preferred in step-growth polymerization due to an increased likelihood of cyclization, we were surprised to find that this was not an issue in our case, likely due to the relatively high weight concentration of PEGDA.

Finally, to demonstrate the utility of oxygen tolerance, we conducted PET-RAFT step-growth at ultralow volume using a 96 well-plate (Figure 4C; Figure S1B, Supporting Information). We conducted the polymerization at 0.5 M monomer concentration, as this was kinetically more optimal for open-air conditions. Pleasingly, the polymerization proceeded to follow the expected step growth molecular weight evolution with conversion accordingly to Flory's theoretical equations (Figure 4D; Table S10, and Figures S33, S36–S37, Supporting Information).[20] Interestingly, the reaction mixture phase-separated after 48 h (Figure S38, Supporting Information), which we attribute to the hygroscopic nature of DMSO and increased atmospheric exposure. Despite the water solubility of PEGDA, hydrophobicity of the CTA_2 rendered the step-growth polymer insoluble in water. Indeed, we found the polymer itself to be soluble in fresh DMSO (Figure S39A, Supporting Information); however, when left stirring open to air overnight, the polymer was found to phase separate (Figure S39B, Supporting Information).

Additionally, as we changed the light source to a milder overhead lamp to accommodate the 96-well plate, we conducted controlled experiments at a higher volume in standard scintillation vials open to the air (at both $[CTA]_0$ 2.0 and 0.5 M, where $[ZnTPP]_0$ = 2.50 mM) (Tables S11–S12, Figure S34–S37, Supporting Information). Unsurprisingly, the higher volume polymerization conditions proceeded much slower than the low volume conditions, which we attribute to the lack of penetration depth of the light.

3. Conclusion

In summary, we successfully demonstrated photo-mediated RAFT step-growth polymerization using diacrylate monomers under both catalyst-free conditions (RAFT-iniferter step-growth) and with a photocatalyst (PET-RAFT step-growth). Additionally, we explored the versatility of the polymerization by conducting an in situ graft copolymerization using both PET-RAFT and RAFT-iniferter conditions. Furthermore, leveraging the flexibility in the solvent selection of diacrylate monomers, we were able to investigate the solvent dependency of PET-RAFT step-growth, where the polymerization in TCE proceeded more rapidly in the first 2 h compared to DMF, DMSO, and 1,4-dioxane, which all showed

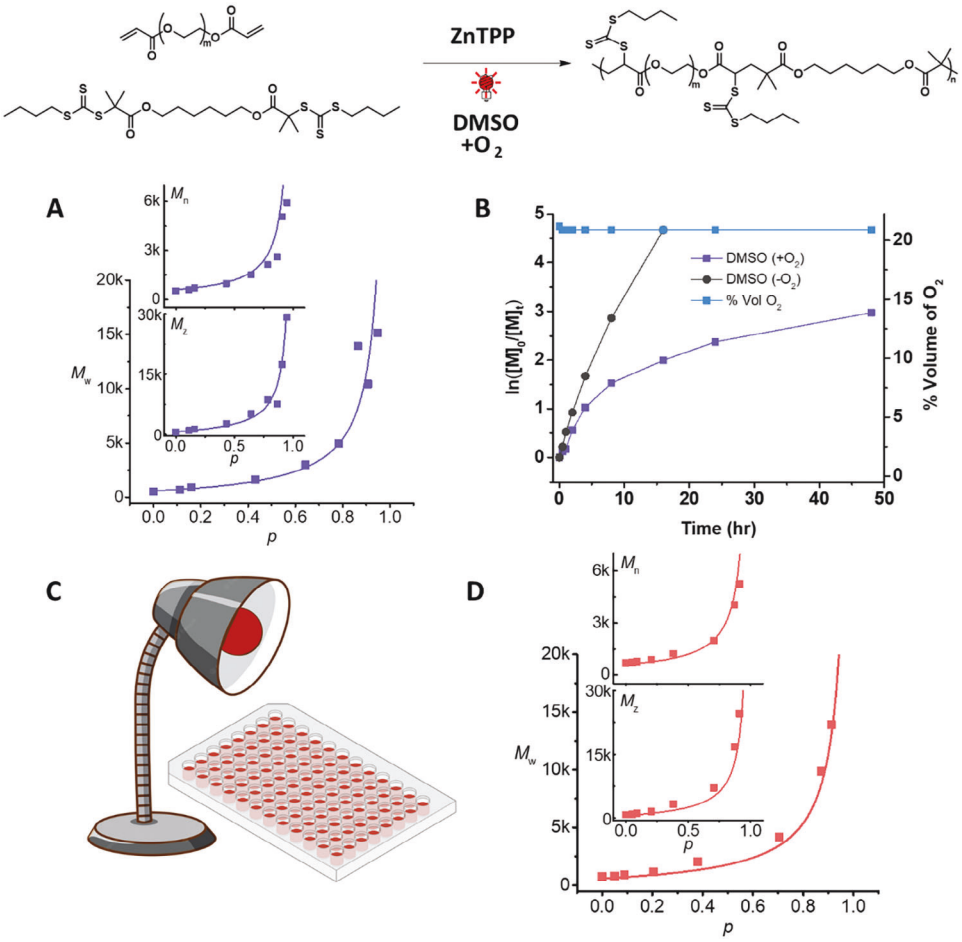

Figure 4. Oxygen tolerant photo-mediated PET-RAFT step-growth polymerization with $\mathbf{M_{2B}}$ and $\mathbf{CTA_2}$ in DMSO. A) Evolution of the molecular weight averages (M_w, M_n, and M_z) from SEC analysis of PET-RAFT step-growth polymerization at Milliliter scale under open-air condition, where $[CTA]_0 = 2.0$ M (Figure S1A, Supporting Information). B) Semi-logarithmic plot of polymerization kinetics for inert gas conditions versus open-air conditions. C) 96-well plate and photoreactor schematic (Figure S1B, Supporting Information). D) Molecular weight evolution of ultralow volume microliter scale PET-RAFT step-growth polymerization under open-air conditions, where $[CTA]_0 = 0.5$ M (Figure S1B, Supporting Information).

comparable linear pseudo-first order kinetics. Lastly, the oxygen tolerance of PET-RAFT step-growth in DMSO allowed us to conduct ultralow volume polymerization under open-air conditions. We demonstrated this capability through a 96-well plate, highlighting the ease and potential for high throughput application.

Supporting Information

Supporting Information is available from the Wiley Online Library or from the author.

Acknowledgements

This work was financially supported by the National Science Foundation (NSF) under Award CHE-2108670. Bruker AVANCE III Nanobay 400 MHz NMR Spectrometer was supported by NSF under Grant No. CHE-0922858, and Bruker NEO 600 MHz NMR spectrometer was supported by NSF under Grant No. CHE-1828183. The authors thank Dr. Marc A. ter Horst from the University of North Carolina's Department of Chemistry NMR Core Laboratory for the use of the NMR spectrometers.

Data Availability Statement

The data that support the findings of this study are available in the supplementary material of this article.

Conflict of Interest

The authors declare the following competing financial interest(s): J.T. and W.Y. are named inventors on a patent application owned by UNC-Chapel Hill (PCT/US2022/042087) which laid the foundation for this work. Dr. You is also a co-founder of Delgen Biosciences, a startup company that has licensed this UNC patent application.

Keywords

oxygen tolerance, photo-mediated, RAFT, step-growth

Received: July 23, 2024
Revised: August 24, 2024
Published online: September 23, 2024

[1] V. A. Bhanu, K. Kishore, *ACS Chemical Reviews* **1991**, *91*, 99.
[2] M. R. Bennett, C. Moloney, F. Catrambone, F. Turco, B. Myers, K. Kovacs, P. J. Hill, C. Alexander, F. J. Rawson, P. Gurnani, *ACS Macro. Lett.* **2022**, *11*, 954.
[3] N. Corrigan, D. Rosli, J. W. Jones, J. Xu, C. Boyer, *Macromolecules* **2016**, *49*, 6779.
[4] A. J. Gormley, J. Yeow, G. Ng, O. Conway, C. Boyer, R. Chapman, *Angew. Chem. Int. Ed. Engl.* **2018**, *57*, 1557.
[5] S. Shanmugam, J. Xu, C. Boyer, *J. Am. Chem. Soc.* **2015**, *137*, 9174.
[6] N. G. Taylor, M. H. Reis, T. P. Varner, J. L. Rapp, A. Sarabia, F. A. Leibfarth, *Polym. Chem.* **2022**, *13*, 4798.
[7] J. Xu, K. Jung, A. Atme, S. Shanmugam, C. Boyer, *J. Am. Chem. Soc.* **2014**, *136*, 5508.
[8] J. Yeow, R. Chapman, J. Xu, C. Boyer, *Polym. Chem.* **2017**, *8*, 5012.
[9] A. Bagheri, C. W. Bainbridge, K. E. Engel, G. G. Qiao, J. Xu, C. Boyer, J. Jin, *ACS Applied Polymer Materials* **2020**, *2*, 782.
[10] G. Szczepaniak, M. Lagodzinska, S. Dadashi-Silab, A. Gorczynski, K. Matyjaszewski, *Chem. Sci.* **2020**, *11*, 8809.
[11] G. Szczepaniak, L. Fu, H. Jafari, K. Kapil, K. Matyjaszewski, *Acc. Chem. Res.* **2021**, *54*, 1779.
[12] X. Dong, L. Wang, Y. He, Z. Cui, P. Fu, M. Liu, X. Qiao, G. Shi, X. Pang, *Polym. Chem.* **2021**, *12*, 7010.
[13] N. Zaquen, A. M. Kadir, A. Iasa, N. Corrigan, T. Junkers, P. B. Zetterlund, C. Boyer, *Macromolecules* **2019**, *52*, 1609.
[14] J. Tanaka, N. E. Archer, M. J. Grant, W. You, *J. Am. Chem. Soc.* **2021**, *143*, 15918.
[15] N. E. Archer, P. T. Boeck, Y. Ajirniar, J. Tanaka, W. You, *ACS Macro. Lett.* **2022**, *11*, 1079.
[16] P. Boeck, N. Archer, J. Tanaka, W. You, *Polym. Chem.* **2022**, *13*, 2589.
[17] S. M. Clouthier, J. Tanaka, W. You, *Polym. Chem.* **2022**, *13*, 6114.
[18] P. T. Boeck, J. Tanaka, W. You, B. S. Sumerlin, A. S. Veige, *Polym. Chem.* **2023**, *14*, 2592.
[19] J. Tanaka, J. Li, S. M. Clouthier, W. You, *Chem. Commun.* **2023**, *59*, 8168.
[20] P. J. Flory, *J. Am. Chem. Soc.* **1936**, *58*, 1877.